Food Control 125 (2021) 107974

Contents lists available at ScienceDirect

Food Control

journal homepage: www.elsevier.com/locate/foodcont

NMR-based metabolomic investigation of antimicrobial mechanism of electrolysed water combined with moderate heat treatment against *Listeria monocytogenes* on salmon

Jiaying Wu [a,b], Lin Zhao [a,b], Shaojuan Lai [c,d], Hongshun Yang [a,b,*]

[a] Department of Food Science and Technology, National University of Singapore, Singapore, 117542, Singapore
[b] National University of Singapore (Suzhou) Research Institute, 377 Lin Quan Street, Suzhou Industrial Park, Suzhou, Jiangsu, 215123, PR China
[c] College of Basic Medicine, Guizhou University of Traditional Chinese Medicine, Guiyang, Guizhou, 550025, PR China
[d] Guangzhou Pulu Medical Technology Co., Ltd, Guangzhou, Guangdong, 510800, PR China

ARTICLE INFO

Keywords:
Heat
Oxidative stress
Foodborne pathogen
Foodomics
Electrolyzed water

ABSTRACT

Heat and acidic electrolysed water (AEW) are considered effective for inactivation of microorganisms. While a previous study elucidated their bactericidal mechanism on *Listeria innocua* through metabolomics *in vitro*, the fundamental mechanism for inaction of *L. monocytogenes* using this method in food system is poorly understood. This work determined the survival population and injury of three *L. monocytogenes* strains (SSA81, LM44, and LM3) inoculated on salmon under heat (60 °C) and AEW (100 mg/L available free chlorine, pH 2.42, oxidation reduction potential 1182 mV) treatments, when applied alone or in combination. The bactericidal mechanism was explored by utilising nuclear magnetic resonance (NMR) and multivariate data analysis. Our results indicated that the individual heat and AEW treatment led to 0.4 and 1.2 log CFU/g reductions of *L. monocytogenes*, respectively. The combined treatment of heat and AEW resulted in notable reductions which were 2.1–2.2 log CFU/g for *L. monocytogenes*. More than 25%, 35%, and 55% injury of *L. monocytogenes* were observed under heat, AEW, and the combined treatment, respectively. Overall, 43 metabolites were characterised in three strains. Short time heat might activate protective system of the cells by accumulating amino acids and organic acids. AEW resulted in the reductions of metabolites due to oxidative and acid stress. In the combined treatment, AEW played the main role and its bactericidal ability was strengthened by heat. Significant decreases of Val, Leu, Tyr, and Trp were detected in all strains under the synergic stress of heat and AEW ($P < 0.05$). There were 15, 7, and 6 pathways, mainly included amino acid, energy, and carbohydrate metabolisms, changed significantly under the combined treatment for SSA81, LM44, and LM3, respectively. The strain LM3 presented the strongest resistance to oxidative stress by the enhancement of Glu decarboxylase system, whereas this compensatory pathway was diminished in SSA81 and LM44. These findings suggest that the bactericidal mechanism can be well explained by disturbed pathways.

1. Introduction

Listeriosis is a potentially fatal foodborne illness caused by *Listeria monocytogenes*, a Gram-positive pathogenic bacterium. The Centers for Disease Control and Prevention (CDC) estimated that in the United States, almost 1600 people suffer from listeriosis every year, leading to 260 deaths. Due to the high mortality rate, government and food safety organisations have implemented serious surveillance and monitoring system (Todd & Notermans, 2011). It has been widely recognised that ready-to-eat (RTE) foods can be contaminated by *L. monocytogenes*. Its presence has been reported in smoked salmon (Josewin et al., 2018), cheese (Park & Ha, 2020), and salads (Lokerse et al., 2016). The strong survival abilities under extremely adverse environments, such as high temperature, low water activities, and acidic pH, make its control challenging (Wang & Shen, 2015).

Salmon is a potential source of contamination and a favourable substrate of *L. monocytogenes*, although the "zero-tolerance" policy, which means no detection of *L. monocytogenes* in either two of the 25 g samples tested, has been established by both Food and Drug Administration (FDA) and Food Safety and Inspection Services (FSIS) (Huang,

* Corresponding author. Department of Food Science and Technology, National University of Singapore, Singapore, 117542, Singapore.
E-mail address: fstynghs@nus.edu.sg (H. Yang).

https://doi.org/10.1016/j.foodcont.2021.107974
Received 24 October 2020; Received in revised form 5 February 2021; Accepted 7 February 2021
Available online 12 February 2021

2017). As a typical *L. monocytogenes* risk food, raw salmon is considered as the initial source of the *L. monocytogenes* contamination route and may cause a potential risk in salmon products (Heir et al., 2020). Because *L. monocytogenes* may colonise and form biofilms on the equipment, processing, packaging, and storage are key risk factors for cross-contamination through contacting with contaminated surfaces or food handlers (Wu et al., 2020). One European-wide survey showed that the prevalence of *L. monocytogenes* in cold-smoked fish samples at retail was up to 17.4% in 2010 and 2011 (Anon, 2013). Schjørring et al. (2017) reported that *L. monocytogenes* contaminated fish was responsible for at least three outbreaks between 2014 and 2017 in Denmark. Miya et al. (2010) indicated that 5.7% of salmon roe was tested positive of *L. monocytogenes* in Japan. Thus, it is important to prevent contamination as the potential growth of the foodborne pathogens on the salmon can cause serious health hazards to consumers.

Many sanitisers, such as chlorine-based sanitisers, organic acids, and essential oils, have been used to inactivate *L. monocytogenes* in seafood industry. As an environmentally friendly, easy to use, and cost-effective sanitiser, acidic electrolysed water (AEW) has been used for sanitising food and food contact surface. Its activity is based on pH, oxidation-reduction potential (ORP), and free available chlorine (FAC) (Huang et al., 2008). In order to improve the antimicrobial ability, AEW is combined with mild heat (Liu, Tan, et al., 2017), ultrasound (Zhao et al., 2017), ultraviolet light (Jiang et al., 2020), or organic acids (Zhao et al., 2019a). The synergy of AEW and a physical treatment or a chemical sanitiser may kill *L. monocytogenes* by the damage of membranes, leakage of intracellular materials, disruption of DNA synthesis, and dysfunction of electron transport system. To date, this synergistic bactericidal effect on cell metabolism is still not well explained.

Previous studies suggested that bacterial metabolism is modulated by gene expression and post-transcriptional and post-translational events. Thus, the metabolomics of cells can potentially reveal the bacterial response to stressors by analysing the global metabolite pool (Ye, Wang, et al., 2012). For instance, Liu et al. (2018) reported the metabolic response of *L. innocua* to AEW stress *in vitro* through the comparison of metabolite profiles. Moreover, metabolite profiles have been used to classify bacterial strains and species. For example, Bundy et al. (2005) distinguished six different *Bacillus cereus* strains through metabolomic profiling. Therefore, metabolomics can monitor the overall results of an environmental stress playing on the cell and present a snapshot of different bacterial strains. Nuclear magnetic resonance (NMR) spectroscopy is a rapid, non-destructive, and informative analysis method commonly used in metabolomics (Li et al., 2020; Lou et al., 2021). Without complicated sample preparation, the compounds in a biological sample can be identified and quantified at a high magnetic field strength (Ye, Wang, et al., 2012). The widely used nuclei methods in NMR-based metabolomics are ^{1}H NMR and ^{13}C NMR. The combination of NMR with multivariate analysis has allowed the differentiation of bacterial strains and the determination of stress response mechanisms of bacteria (Chen, Zhao, Wu, Liu, et al., 2020).

Among the harvested salmon in the United States, 40% of them are converted into the canned or pouched product by retort processing (Kong et al., 2007). Postprocessing intervention plays an important role in the RTE food supply chain because postprocessing contamination may occur after cooking (Zhu et al., 2005). Here, we chose autoclaved salmon as a representative RTE food model and heat and AEW as sanitising methods. Although most research focuses on the evaluation of antimicrobial effects of heat and AEW, the global metabolic response of *L. monocytogenes* to heat and AEW has not been investigated. The main objective of this report was to assess the metabolic changes and disturbed pathways of *L. monocytogenes* under heat, AEW, and their combined treatment. Initially, survival population and percentage of injury after treatments were evaluated. To investigate underlying mechanism behind treatments, we interpreted cellular chemical fingerprints based on identification and quantification of metabolites using NMR spectroscopy. In addition, the metabolic profiles, principle metabolites, and affected pathways under treatments were determined through multivariate data analysis.

2. Materials and methods

2.1. Materials and treatment solutions

Deionised water (DW) was generated by a Mill-Q purification system. Tryptone soya broth (TSB), tryptone soya agar, yeast extract, phosphate buffer saline (PBS, pH 7.2), peptone water, sodium chloride, sodium thiosulfate, and sodium 3-trimethylsilyl [2,2,3,3-d4] propionate (TSP) were obtained from Sigma-Aldrich (Singapore). Neutralising buffer (formula: 0.0425 g/L monopotassium phosphate; 0.16 g/L sodium thiosulfate; 5.0 g/L aryl sulfonate complex) was purchased from Becton, Dickinson and Company (Sparks, MD, USA). Acidic electrolysed water (AEW) was generated by electrolysis of 0.9% sodium chloride solution in an electrolysis device (Hoshizaki, ROX-10WB3, Hoshizaki Singapore Pte Ltd, Singapore). The pH, FAC, and ORP were measured using a pH meter (Thermo Orion pH meter, Waltham, MA, USA), a chlorine test kit and RQflex® 10 Reflectoquant® (Merck, Darmstadt, HE, Germany), and an ORP meter (HM Digital ORP-200, Culver City, CA, USA), respectively.

AEW was collected into a sterile glass bottle and used within 1 h postproduction in order to avoid the loss of chorine. Sterilised DW was used to dilute AEW to obtain the FAC of 100 mg/L (ORP 1182.0 ± 30.8 mV, pH 2.42 ± 0.13). To test FAC, AEW was initially measured semi-quantitatively by visual comparison of the test strip with a colour scale. After that, AEW was diluted to less than 10 mg/L FAC to fit the measuring range of reflectometer. The test strip was immersed into diluted AEW for 2 s and immediately inserted into the strip adapter of reflectometer for quantitative reading. For heat treatment, capped glass bottle containing treatment solution was put in a water bath at 60 °C.

2.2. Bacterial strains and culture conditions

Three *L. monocytogenes* strains, namely, SSA81 (serotype 1/2a), LM44 (serotype 3a), and LM3 (serotype 4b) that were initially isolated from smoked salmon, were obtained from the Department of Food Science & Technology, National University of Singapore. The strains, which were kept at −80 °C, were activated in 5 mL sterile TSB at 37 °C for 24 h. A loopful of cell suspension was streaked on tryptone soya agar with 0.6% (w/v) yeast extract (TSAYE) and incubated at 37 °C for 48 h to isolate a single colony. An individual colony was inoculated in 10 mL TSB and subcultured twice at 37 °C for 24 h. The cultures were centrifuged (8000×*g*, 10 min, 20 °C). The resulting pallets were washed twice in 10 mL 0.1% (w/v) peptone water. Washing was done by re-suspending the cells followed by centrifuged (8000×*g*, 10 min, 20 °C). Washed cells were then re-suspended in 10 mL peptone water. The obtained suspensions were diluted (1:10, v/v) to about 6.5 log CFU/mL for following inoculation procedure.

2.3. Inoculation on salmon cubes

Freshly packed Norwegian farmed Atlantic skinless salmon fillets were obtained from a supermarket in Singapore. All fillets were sliced into cubes and autoclaved (15 min, 121 °C). After cooling down inside of the biosafety cabinet, the salmon cubes were briefly rinsed in sterile DW and air-dried for 30 min. Weighed salmon cubes (3.0 ± 0.2 g) were inoculated with *L. monocytogenes* by spotting 30 μL of the prepared suspension on each side of the cubes (Chhetri et al., 2019). Three *L. monocytogenes* strains were inoculated separately. Each strain was inoculated on four salmon cubes for four different treatments. The inoculated samples (about 4.5 log CFU/g) were placed in glass baking dishes without cover (one dish per sample) and kept inside the biosafety cabinet to enable the growth of *L. monocytogenes* on salmon under room temperature (25 °C). After 24 h, final concentration of *L. monocytogenes* was about 8.0 log CFU/g in salmon.

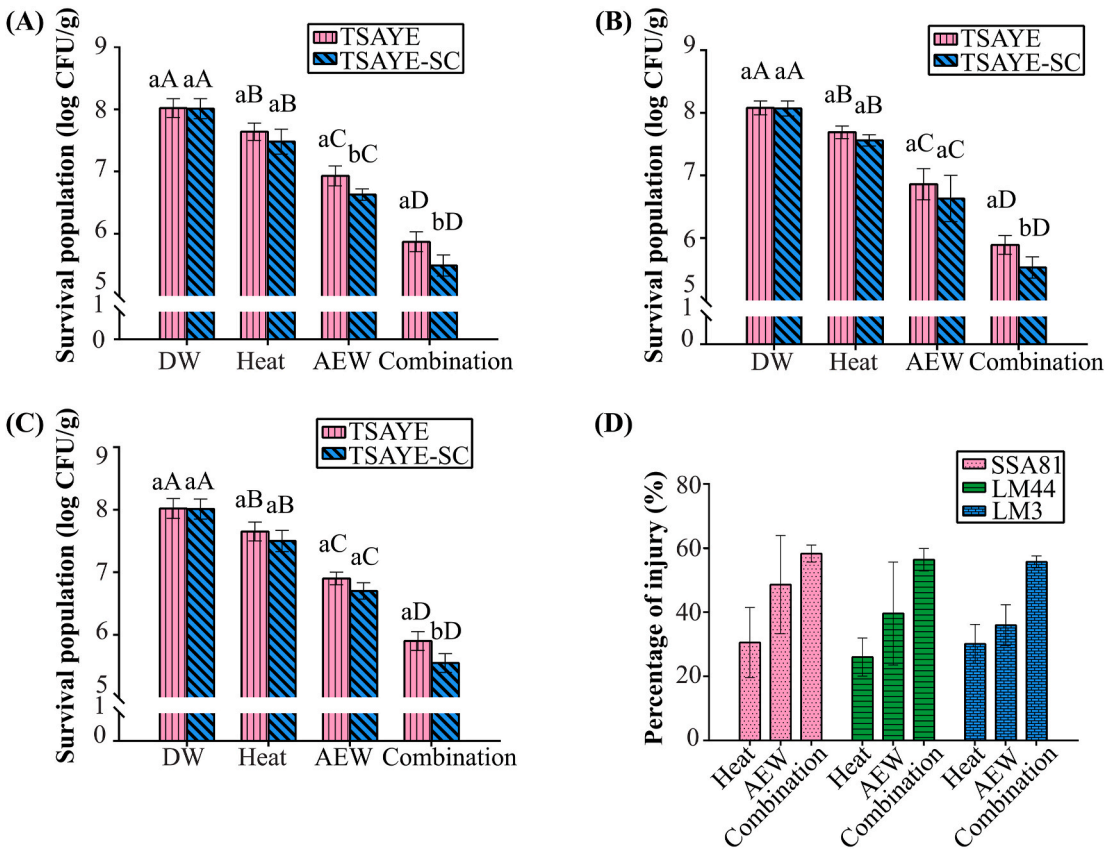

Fig. 1. The survival populations of SSA81 (A), LM44 (B), LM3 (C), and the percentage of injury (D) under treatments. Data are displayed as means ± standard deviation. Different lowercase letters represent statistical differences between tryptone soya agar with 0.6% (w/v) yeast extract and tryptone soya agar with 0.6% (w/v) yeast extract and 5% (w/v) sodium chloride with the same treatment. Different capital letters represent statistical differences between different treatment methods with the same media.

2.4. Sanitising treatments

The inoculated salmon cubes were divided into four treatment groups: (I) DW (20 °C, DW as solution); (II) heat (60 °C, DW as solution); (III) AEW (20 °C, AEW as solution); (IV) the combination of heat and AEW (60 °C, AEW as solution). For heat (II) and the combined treatment (IV), the treatment solutions were heated to 60 °C in advance. Samples were immersed into 27 mL treatment solutions for 5 min. After that, 30 mL neutralising buffer containing sodium thiosulfate was added to stop the sanitisation treatment by neutralising the residual chlorine and acidity (Shen et al., 2019). The salmon cubes were then homogenised (Masticator Stomacher, IUL Instruments, Germany) in the neutralised treatment solution for 1 min before microbiological analysis (Krajnik et al., 2017).

2.5. Microbiological analysis

Microbiological analysis was conducted by bacterial count enumeration performed on selective and non-selective media. To enumerate colonies from both injured and uninjured cells, TSAYE was used as non-selective media. On the other hand, TSAYE with 5% (w/v) sodium chloride (TSAYE-SC) served as selective media for growth of uninjured cells into colonies (Lan et al., 2019). Peptone water was used for decimal dilution and 100 μL of diluent was plated on both media. After incubation (37 °C, 48 h), the cell population was enumerated and presented by log CFU/g salmon cubes. The percentage of injury after treatments were calculated based on the following equation:

The percentage of injured cells (%) = [1- (count on TSAYE-SC/count on TSAYE)] *100%

2.6. Extraction of L. monocytogenes metabolites

Each of three *L. monocytogenes* strains was conducted individually. In order to obtain enough *L. monocytogenes* cells for the extraction of metabolites, a total of 800 g salmon cubes was used for the inoculation in each group. After treatment with DW (I), heat (II), AEW (III), and the combination of heat and AEW (IV) for 5 min, the cells were re-suspended by triturating with a pipette (Dupre et al., 2019). Cell suspensions were centrifuged at low speed (1500×*g*, 3 min, 4 °C) to precipitate debris (Zhao et al., 2020). After centrifuging at high speed (12,000×*g*, 10 min, 4 °C), the pelleted cells were washed two times using PBS and then suspended in 5 mL extraction solution. Extraction solution comprised a mixture of the same volumes of NaH_2PO_4–K_2HPO_4 buffer and acetonitrile. The samples were immersed in ice and sonicated for 25 cycles with 5 s pulses and 10 s stop. The lysed cells were centrifuged (12,000×*g*, 10 min, 4 °C) and the metabolites were collected with the supernatant in a clean tube. To the cell residues, 5 mL of extraction solutions was added. The mixture was homogenised by vortex and centrifuged at the same condition to obtain the secondary supernatant. Rotary evaporation was used to remove water and acetonitrile in the combined supernatants. The resulting samples were subject to NMR analysis.

2.7. NMR spectroscopic analysis

The obtained metabolites were dissolved in 600 μL deuterated water (D_2O, 99.9%) with 0.005% TSP (internal standard) and pipetted into NMR tubes. NMR experiments were conducted at 298 K by a Bruker DRX-500 NMR Spectrometer with a Triple Inverse Gradient (TXI) probe (Bruker, Germany). The parameters for ^1H NMR were set based on the previous method (Liu, Wu, et al., 2017; Liu et al., 2018; Zhao et al.,

2019c). Briefly, for all samples, standard Bruker NOESY pulse sequence (recycle delay-90°-t_1-90°-t_m-90°-acquisition) was applied. Water suppression was measured during both the recycle delay (RD, 2s) and the mixing time (t_m, 100 ms) by using a weak continuous wave irradiation. Sixty-four induction decays were collected with a spectral width of 20 ppm and an acquisition time of 1.36 s into 32 k data. All free induction decays were transformed by an exponential window function with a broadening factor of 1 Hz before Fourier transformation (FT). For the qualification of metabolites, the 2D ^{1}H–^{13}C heteronuclear single quantum coherence spectroscopy (HSQC) of one *L. monocytogenes* sample was obtained using the Bruker hsqcedetgpsisp2.3 pulse sequence at 298 K. The ^{1}H spectra with a width of 10 ppm and the ^{13}C spectra with a width of 180 ppm were tested in the F2 and F1 channel, respectively.

2.8. Spectral analysis

The 1D ^{1}H spectra were subject to TopSpin 3.6.0 (Bruker) to correct baseline, phase, and TSP signal manually. The 1D ^{1}H NMR spectra were used to quantify the metabolites based on the known concentration of internal standard (TSP) as the intensities of compounds on NMR spectra were correlated linearly with their concentrations. The 2D ^{1}H–^{13}C NMR were used to identify metabolites by analysing the peaks on the ^{13}C spectra and ^{1}H spectra cooperatively. Software Mnova (Mestreab, Research SL, Santiago de Compostela, Spain) was utilised to exclude the water region (4.76–4.79 ppm) and normalise peaks from 0.5 to 10.0 ppm to sum intensities. The region bucket was divided into 0.01 ppm and binned data were collected for further processing.

SIMCA software (version 13.0, Umetrics, Umeå, Sweden) was used to conduct multivariate analysis. The principal component analysis (PCA) and orthogonal projection to latent structure discriminant analysis (OPLS-DA) were used to separate groups and identify responsible compounds, respectively. Based on binned data, the fold changes (FCs) and related *P* values of pairwise groups were calculated. The pathway analysis and interpretation were conducted by MetaboAnalyst 4.0 (http://www.metaboanalyst.ca/). and Kyoto Encyclopedia of Genes and Genomes (KEGG) database (https://www.genome.jp/kegg/pathway.html) cooperatively.

2.9. Statistical analysis

Each experiment was conducted at least in triplicates independently. The results of microbiological analysis were converted into log CFU/g counts on salmon. The survival population and percentage of injury were expressed as mean ± standard deviation. Analysis of variance (ANOVA) and the least significant difference (LSD) were conducted by SAS software (version 9.2, Cary, NC, USA) to compare the survival population under different treatments. Differences with $P < 0.05$ were regarded as significant.

3. Results and discussion

3.1. Survival population and percentage of injury of L. monocytogenes after treatments

The antimicrobial effects of three *L. monocytogenes* strains under DW, heat, AEW, and the combined treatment of heat and AEW were determined by enumerating colonies on TSAYE and TSAYE-SC. Fig. 1 shows the survival population and percentage of injury of three *L. monocytogenes* strains under treatments. Overall, the population of three *L. monocytogenes* strains before treatments was approximately 8.0 log CFU/g. Similar trends were observed for three *L. monocytogenes* strains. The combined treatment of AEW and heat exhibited the best antimicrobial effect, with 2.1–2.2 log CFU/g reductions on TSAYE for all the three strains of *L. monocytogenes*. As shown in Fig. 1A–C, for three *L. monocytogenes* strains, the significant differences ($P < 0.05$) between control, heat, AEW, and the combined groups were found on both TSAYE and TSAYE-SC. There was no significant difference ($P > 0.05$) between TSAYE and TSAYE-SC cell counts in the control and heat groups. In samples treated with the combination of heat and AEW, the population on TSAYE was higher ($P < 0.05$) than on TSAYE-SC. Under AEW treatments, the survival population of SSA81 on TSAYE-SC was lower ($P < 0.05$) than TSAYE, whereas there were no significant differences ($P > 0.05$) for LM44 and LM3.

Three *L. monocytogenes* strains presented similar trend of percentage of injury under treatments. Heat treatment led to the lowest percentage of injured cells (26.0–30.6%), followed by AEW treatment (36.0–48.6%), while the combination of heat and AEW resulted in the highest percentage of injured cells (55.7–58.3%). The percentage of injured SSA81 cells under the combined treatment was 58.3%, which was higher than LM44 (56.4%) and LM3 (55.7%) (Fig. 1D). The results indicated that SSA81 was more susceptible than LM44 and LM3 under the combination of AEW and heat. Our results were consistent with the study by Liu et al. (2020), which indicated that the combination of heat and electrolysed water produced better inactivation effects than individual treatment. They also reported different survival abilities of two strains *E. coli* (O157:H7 EDL933 and ATCC 25922) under the same treatment.

Similarly, Shiroodi et al. (2016) reported that AEW (60 mg/L FAC, pH 2.7, ORP 1150 mV) treatment for 10 min at 20 °C resulted in 1.6 log CFU/g reductions of *L. monocytogenes* ATCC 19114 on cold-smoked Atlantic salmon. Krajnik et al. (2017) indicated that AEW (65 mg/L FAC, pH 2.6, ORP 1140 mV) treatment for 1 min reduced 0.2 log CFU/g of *L. monocytogenes* cocktail on salmon. Because the injured bacteria can resuscitate and rejuvenate in a suitable environment and develop stress resistance, food products with injured pathogens may increase the risk of foodborne illness. Izumi and Inoue (2018) indicated that the injured bacteria recovered quickly because of the elevated level of metabolism and the improved adaptability of toxic oxygen radicals. Thus, the metabolic response of injured *L. monocytogenes* was further evaluated in our study.

3.2. Metabolic profiles of L. monocytogenes strains

Based on three NMR databases, namely, Biological Magnetic Resonance Data Bank (http://www.bmrb.wisc.edu/), Madison Metabolomics Consortium Database (http://mmcd.nmrfam.wisc.edu/), and Human Metabolome Database (http://www.hmdb.ca/), 1D ^{1}H and 2D ^{1}H–^{13}C NMR spectra were analysed cooperatively. Related studies which identified metabolites using NMR-based methods were also used as references (Liu et al., 2018; Ye, Wang, et al., 2012). Table S1 shows a total of 43 metabolites with assignment of peaks by ^{1}H and ^{13}C chemical shifts. The representative ^{1}H NMR spectra with the assignment of signals of three *L. monocytogenes* strains are shown in Fig. S1 and Fig. S2.

The metabolites of three *L. monocytogenes* strains, including amino acids, alcohols, organic acids, sugars, nucleotides, and other derivatives, displayed high similarity. The majority of signals in 0.5–5.5 ppm belonged to amino acids (Ile, Cys, Leu, Val, Ala, Thr, Met, Glu, Asp, and Gly), organic acids (lactic acid, acetic acid, succinic acid, pyruvic acid, and oxoglutaric acid), and sugar (fructose-6-phosphate and glucose-6-phosphate). Two alcohols, ethanol and 1,2-propanediol, also appeared in this region. From 5.5 to 10.0 ppm, nucleotides (ADP, Cyclic AMP, and ATP) and others (putrescine, betaine, NAD, and NADP) contributed the main signals.

Slight differences in intensity and diversity were observed among three *L. monocytogenes* strains in the control group. For example, the intensity of Asp in SSA81 was weaker than that in LM44 and LM3, whereas putrescine was stronger in SSA81 than that in LM44 and LM3. Moreover, betaine had higher intensity in LM44 than that in LM3, whereas glucose-1-phosphate level was lower in LM44 than that in LM3. Interestingly, ethanol occurred in the control group of SSA81 but not in LM44 and LM3. Our results indicated that metabolic profile showed strain specificity and can be used to characterise *Listeria* strains. Lungu

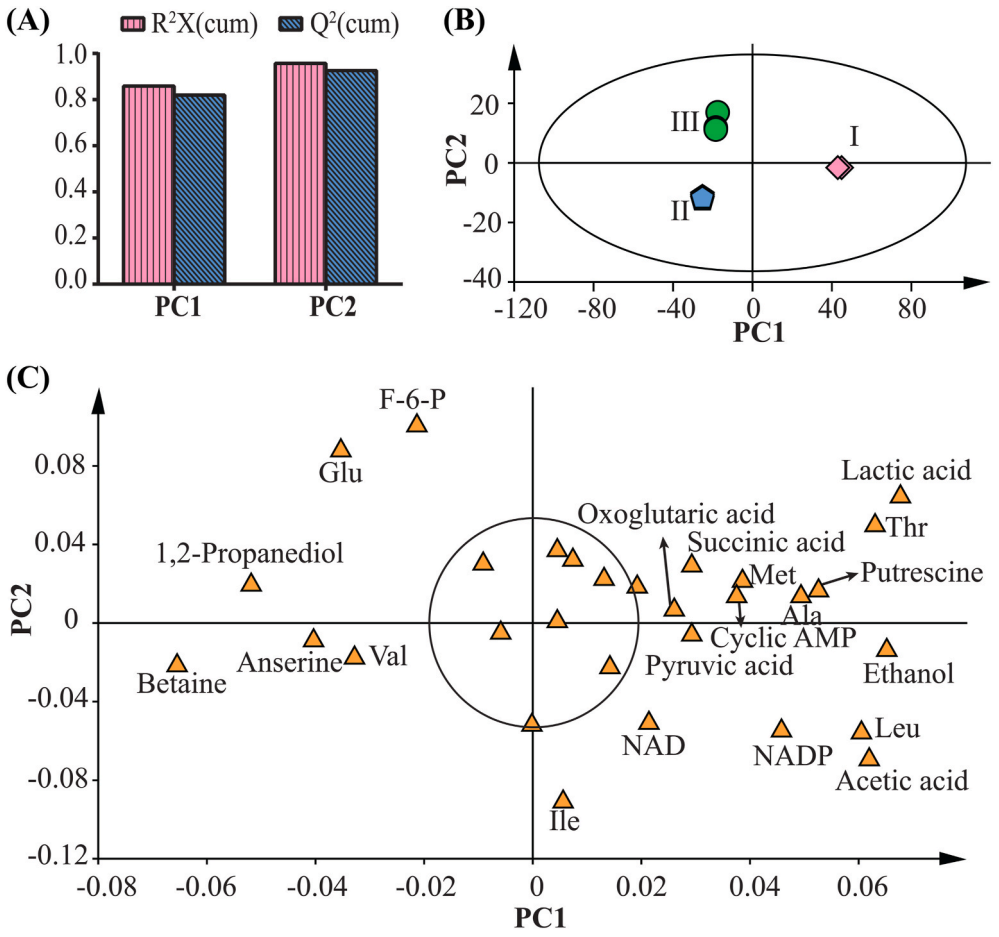

Fig. 2. Principal component analysis (PCA) of ^{1}H NMR spectra of three *Listeria monocytogenes* strains in the control groups. The variances are explained by principal components in PCA (A); the score plot of PCA (B); the loading plot of PCA (C). Note: I: SSA81; II: LM44; III: LM3.

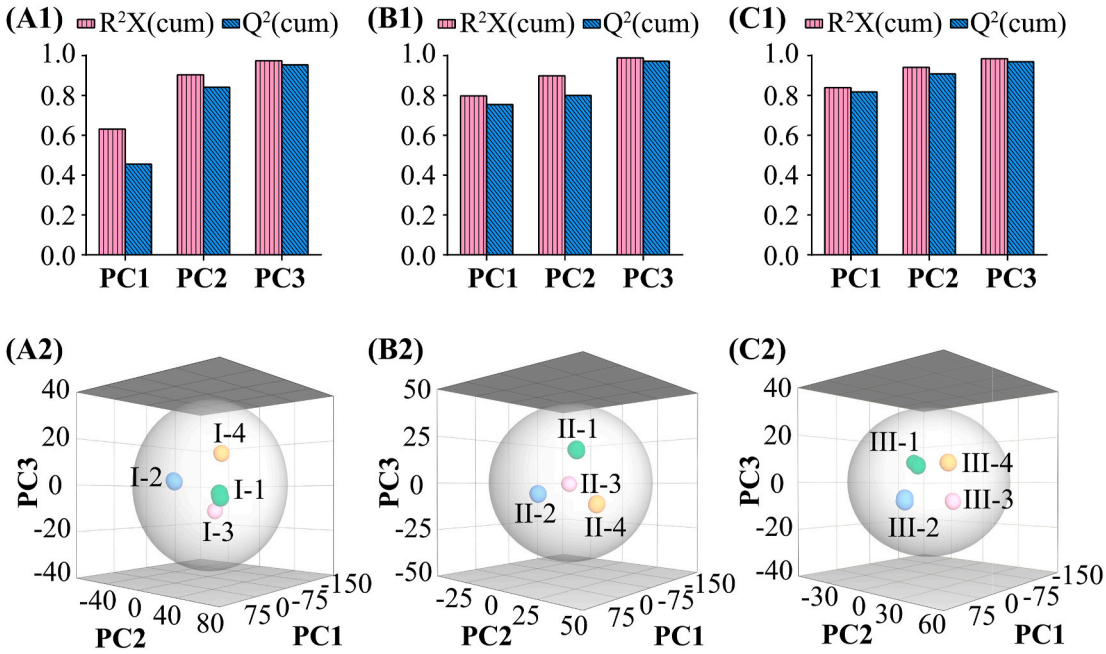

Fig. 3. Principal component analysis (PCA) of ^{1}H NMR spectra of *Listeria monocytogenes* strains under different treatments. The variances are explained by principal components in PCA (A1-C1); the score plot of PCA (A2-C2). Note: I: SSA81; II: LM44; III: LM3; 1: DW treatment; 2: heat treatment; 3: AEW treatment; 4: combination of heat and AEW treatment.

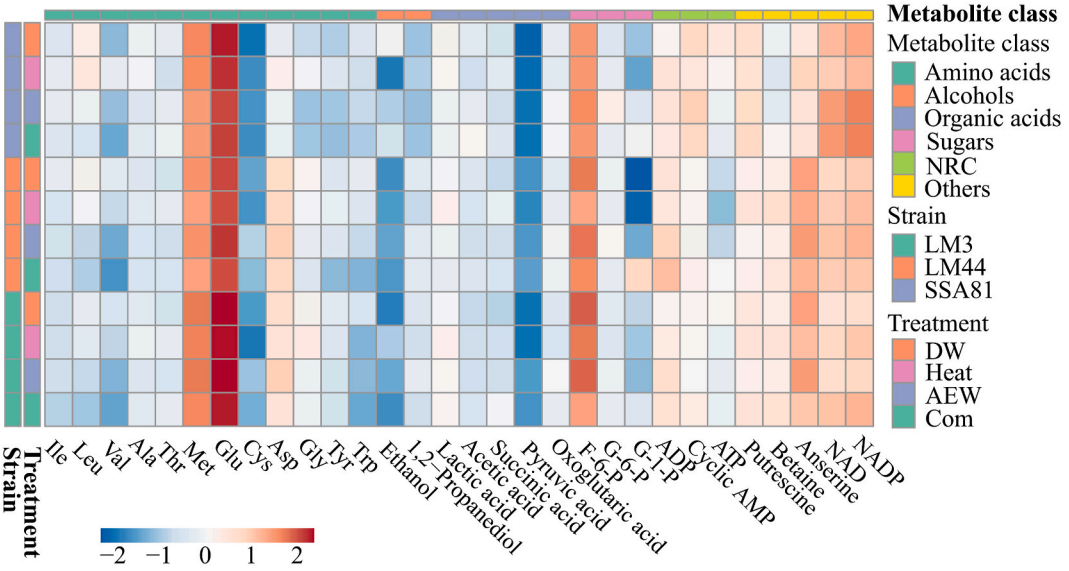

Fig. 4. Heatmap of metabolites in *Listeria monocytogenes* strains under heat, acidic electrolysed water (AEW), and their combined treatment. Note: NRC: nucleotide-related compounds; Com: combination of heat and AEW treatment.

et al. (2009) indicated that individual strains presented characteristic media requirements, sugar, and energy metabolisms.

3.3. Comparison of metabolites in L. monocytogenes strains

To further understand the differences among three *L. monocytogenes* strains, PCA was utilised to analyse discrepancies between metabolomes, investigate the group discriminations, and identify the metabolites associated with different strains. Fig. 2 presents the model quality, grouping information, and discriminative metabolites by R^2X and Q^2, score plot, and loading plot, respectively.

Fig. 2A shows that PC1 and PC2 revealed 95.7% of overall dataset (PC1: 85.9%; PC2: 9.8%) and the Q^2 value (0.93 > 0.50) revealed the good predictability of this model. Through visual inspection, *L. monocytogenes* strains were well separated by the first two PC and clustered into three parts on the score plot (Fig. 2B). The SSA81

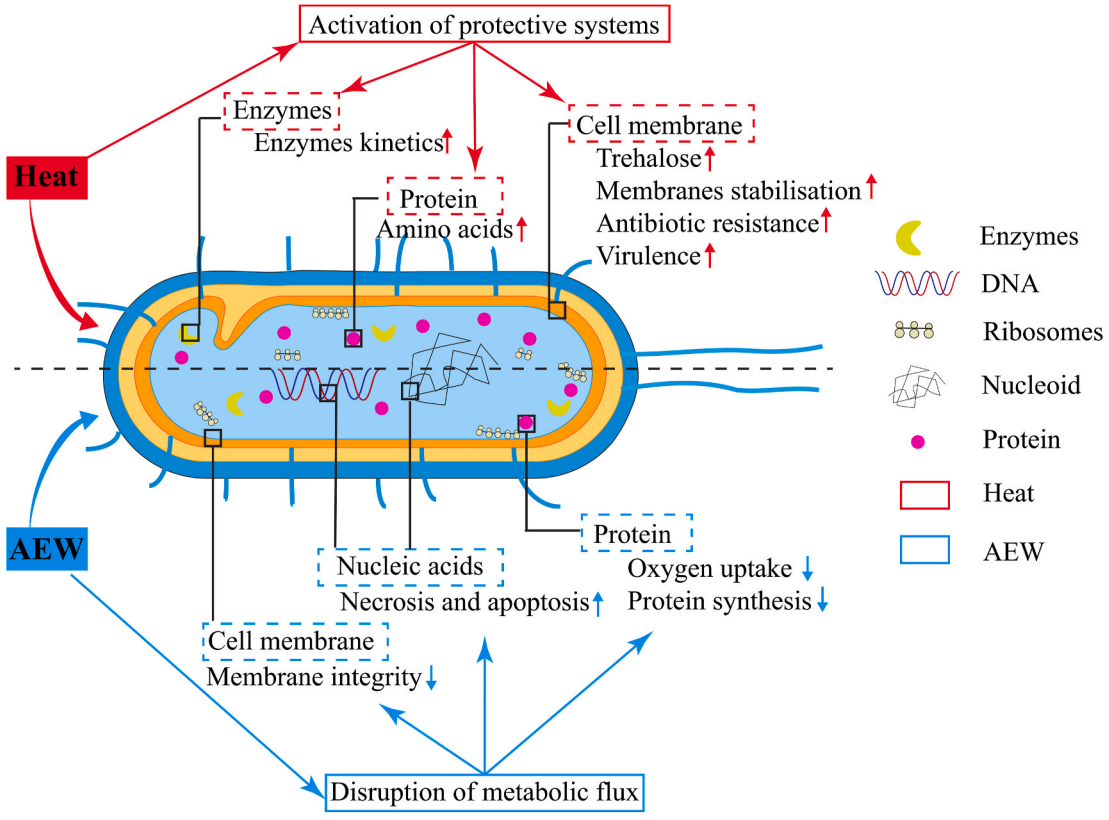

Fig. 5. Proposed mechanisms of bactericidal effects of heat and acidic electrolysed water (AEW) treatments. Note**:** The mechanisms related to heat and AEW are showed in red and blue box, respectively. (For interpretation of the references to colour in this figure legend, the reader is referred to the Web version of this article.)

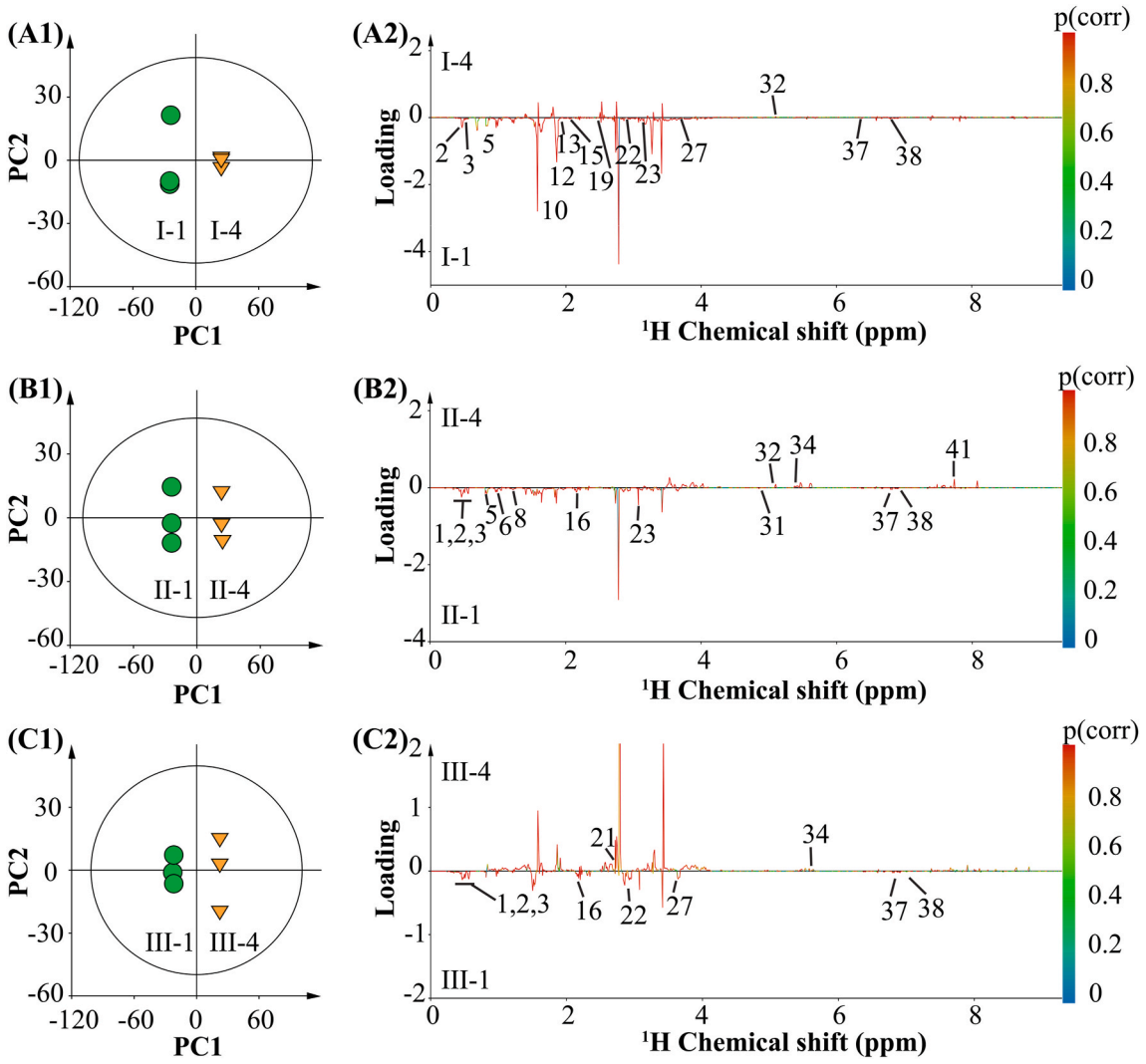

Fig. 6. Orthogonal projection to latent structure discriminant analysis (OPLS-DA) for the control and combined treatment groups. The score plot of OPLS-DA (A1-C1); Loading S-line (A2-C2). Note: I: SSA81; II: LM44; III: LM3; 1: DW treatment; 4: combination of heat and AEW treatment.

appeared at the right side of PC1, while LM44 and LM3 appeared at the left side of PC1 but with opposite PC2 values (Table S2). This indicated the metabolic profiles of three *L. monocytogenes* strains were different. The discriminative metabolites among three *L. monocytogenes* strains are shown in loading plot (Fig. 2C). Metabolites such as Leu, Val, Ala, Thr, Met, ethanol, lactic acid, putrescine, pyruvic acid, anserine, oxoglutaric acid, betaine, and 1,2-propanediol characterised PC1 while Ile, Glu, Tyr, acetic acid, and fructose-6-phosphate represented PC2 (Table S3). The results revealed that metabolomics is an effective method for differentiation of bacterial strains and discovery of potential biomarkers.

3.4. Principal components analysis of L. monocytogenes strains under treatments

PCA was constructed for each *L. monocytogenes* strains using the first three components (PC1, PC2, and PC3) to show the overall metabolites discrimination under DW, heat, AEW, and the combined treatments. Fig. 3 shows the model quality and clustering information of three strains. For SSA81, the first three components explained 97.5% of total variance (PC1: 63.2%; PC2: 27.2%; PC3: 7.1%) (Fig. 3A1). For LM44, the first three components explained 98.9% variances with PC1 explaining 79.8% and PC2 explaining 10.0% of the variances (Fig. 3B1). For LM3, PC1, PC2, and PC3 explained 83.9%, 10.2%, and 4.3%, respectively (Fig. 3C1). The Q^2 values were 0.95, 0.97, and 0.97 for SSA81, LM44, and LM3, respectively. Overall, the parameters, R^2X and Q^2, revealed the good model quality with high interpretative ability and predictability (Zhao et al., 2020). The samples of each *L. monocytogenes* strain were separated with four treatments but clustered under the same stress in score plot (Fig. 3A2-C2). The results suggested that *L. monocytogenes* displayed different sensitivities, tolerances, and metabolic responses to heat, AEW, and the combination of both treatments.

3.5. Alternative metabolites during the individual treatment of heat or AEW

To further understand detailed metabolic changes under each stress, a total of 30 metabolites with characteristic chemical peaks were quantified in a heatmap. Fig. 4 presents the metabolites concentration by using $\log_{10}$ transformation. The deeper blue and red colour on the heatmap illustrated the lower and higher concentration of metabolites, respectively. Overall, our findings were in accord with a past study which analysed the concentration of metabolites present in *L. monocytogenes* strain 10403S (serotype 1/2a), with Glu as the most abundant amino acids and lactic acid as the most abundant organic acids among detected metabolites (Singh et al., 2011).

The similar results were observed on three *L. monocytogenes* strains under heat and AEW treatments individually. On the one hand, our

results indicated that the concentration of ADP, majority of amino acids (Ile, Leu, Ala, Glu, and Gly), and organic acid (succinic acid, pyruvic acid, and oxoglutaric acid) were elevated after heat treatment. Fig. 5 indicates the proposed mechanism for this method. One probable reason is the activation of protective systems in cells by heat shock, leading to accumulation of amino acids and ability of resistance. For example, trehalose, a compound that can response biological stress and regulate metabolic pathways, can be synthesised when cells are exposed to heat, osmotic stresses, and oxidative stress (Cejka et al., 2019). A high level of trehalose contributes to cell protection through membranes stabilisation, inducing antibiotic resistance and virulence in pathogens (MacIntyre et al., 2020). Moreover, in order to maintain the homeostasis, the modulated enzyme kinetics under heat stress may drive desirable reactions and regulate metabolic pathways within the cells. In addition, due to thermoprotective properties of some metabolites, such as Glu, protein disaggregation and refolding can occur under high temperature (Diamant et al., 2001).

On the other hand, AEW treatment inhibited the production of major metabolites in *L. monocytogenes* strains, such as most amino acids (Ile, Leu, Val, Ala, Thr, Met, Glu, etc.), alcohols (ethanol, 1,2-propanediol), and organic acids (lactic acid, acetic acid, succinic acid, etc.). The proposed mechanism is shown in Fig. 5. In AEW, the major chlorine compounds which closely related with pH and ORP, such as hypochlorous acid (HOCl) and hypochlorite ions (OCl^-), may damage membrane integrity, penetrate cells, inhibit glucose oxidation, lower oxygen uptake, and disrupt metabolic flux and protein synthesis (Hati et al., 2012; Len et al., 2000). In addition, the redox state of the cell could be damaged by oxidative species present in AEW, such as hydrogen peroxide (H_2O_2) and superoxide anion ($\cdot O_2^-$), resulting in the necrosis and apoptosis of pathogens (Liao et al., 2007). Overall, the reactive groups in cells, such as amino groups and peptide bonds, displayed high sensitivity to AEW, leading to negative metabolic reaction and metabolites changes (Zhao et al., 2019b).

Interestingly, discrepancies in the amount of several metabolites were observed in different strains. For instance, compared with their respective control groups, the amount of betaine in SSA81 decreased under heat treatment whereas it was increased in LM44 and LM3. Under AEW treatment, glucose-1-phosphate presented with higher amount in SSA81 and LM44 than that in LM3. The detected accumulation and depletion of metabolites indicated that although there are similarities in how different *L. monocytogenes* serotypes respond to environmental stresses, they also exhibit characteristics of individual strains. Faleiro et al. (2003) reported different sensitivities to acid and sodium chloride in four *L. monocytogenes* strains isolated from cheese. This behaviour of bacteria can be ascribed to the strain specific differences in response to the stresses (Alighialo et al., 2019).

3.6. Alternative metabolites during the combined treatment of heat and AEW

Having demonstrated the metabolic changes of three *L. monocytogenes* strains under heat or AEW treatments individually, we then investigated the response of *L. monocytogenes* to the combined treatment of heat and AEW. The OPLS-DA was conducted based on the control and combined groups of each *L. monocytogenes* strain and evaluated by R^2X and Q^2. Fig. 6 shows the OPLS-DA results of the control and combined groups. The score plot and S-line of each strain were used to visualise separations between groups and to determine the metabolites responsible to the separation, respectively. All the models exhibited clear separation and reliable predictability (SSA81: $R^2X = 0.898$, $Q^2 = 0.995$; LM44: $R^2X = 0.842$, $Q^2 = 0.997$; LM3: $R^2X = 0.776$, $Q^2 = 0.992$). As shown in Fig. 6A1-C1, the well separated control and combined groups indicated that the metabolic profiles significantly changed after the combined treatment.

The S-line provided clear views of the compounds responsible for metabolic differences. Downward peaks illustrated detected metabolites with the lower concentration in the combined treatment group compared to the control group, vice versa. Most metabolites in SSA81, such as Leu, Val, Glu, and succinic acid reduced significantly under the combined treatment while glucose-1-phosphate was elevated (Fig. 6A2). The S-line of LM44 showed that the combined treatment increased glucose-1-phosphate, ADP, and ATP and decreased Ile, Leu, Val, and anserine (Fig. 6B2). For LM3, higher concentration of betaine and ADP was detected in the combined group (Fig. 6C2). However, the concentration of Ile, Leu, Val, Trp, Tyr, anserine, 1,2-propanediol, and fructose-6-phosphate in the combined group was lower than that in the control group (Fig. 6C2). Our results indicated that majority of the compounds reduced under the combination of heat and AEW treatment. The amino acids were the primary targets. A previous study that evaluated metabolic response of *E. coli* to electrolysed water showed similar results (Liu, Wu, et al., 2017).

Table 1
Fold changes of metabolites in three *Listeria monocytogenes* strains after the combination of heat and acidic electrolysed water (AEW) treatments.

Metabolites	Fold changes × 10^{-1}		
	SSA81	LM44	LM3
Ile	8.27 ± 0.03^{a}	2.94 ± 0.01^{c}	5.83 ± 0.09^{b}
Leu	3.16 ± 0.01^{bz}	2.36 ± 0.01^{c}	4.34 ± 0.05^{a}
Val	4.83 ± 0.10^{a}	0.76 ± 0.02^{c}	2.42 ± 0.04^{b}
Ala	6.72 ± 0.12^{b}	6.30 ± 0.06^{b}	11.20 ± 0.39^{a}
Thr	7.23 ± 0.01^{b}	13.93 ± 0.27^{a}	13.23 ± 0.55^{a}
Met	5.14 ± 0.04^{c}	7.12 ± 0.11^{b}	10.60 ± 0.07^{a}
Glu	6.18 ± 0.03^{c}	7.03 ± 0.11^{b}	10.87 ± 0.16^{a}
Cys	7.19 ± 0.09^{a}	9.38 ± 0.83^{a}	8.75 ± 1.86^{a}
Asp	8.70 ± 0.17^{a}	8.84 ± 0.99^{a}	9.21 ± 0.79^{a}
Gly	6.47 ± 0.05^{b}	6.10 ± 0.76^{b}	9.12 ± 0.35^{a}
Tyr	4.90 ± 0.10^{b}	1.67 ± 0.07^{c}	6.27 ± 0.11^{a}
Trp	3.67 ± 0.07^{a}	1.82 ± 0.16^{c}	3.02 ± 0.10^{b}
Ethanol	4.86 ± 0.48^{c}	6.90 ± 1.07^{b}	9.22 ± 0.45^{a}
1,2-Propanediol	6.32 ± 0.06^{b}	6.89 ± 0.04^{a}	5.19 ± 0.07^{c}
Lactic acid	4.82 ± 1.19^{b}	5.70 ± 0.33^{b}	11.69 ± 4.11^{a}
Acetic acid	10.32 ± 0.04^{b}	8.49 ± 0.14^{c}	14.72 ± 0.16^{a}
Succinic acid	5.45 ± 0.05^{c}	8.72 ± 0.30^{b}	9.82 ± 0.15^{a}
Pyruvic acid	6.26 ± 0.01^{c}	8.73 ± 0.55^{b}	12.00 ± 0.17^{a}
Oxoglutaric acid	6.52 ± 0.22^{b}	9.78 ± 0.44^{b}	9.92 ± 0.52^{a}
F-6-P	5.76 ± 0.06^{b}	7.58 ± 0.08^{a}	4.65 ± 0.58^{c}
G-6-P	11.31 ± 1.13^{a}	3.08 ± 0.69^{c}	8.40 ± 1.87^{b}
G-1-P	23.83 ± 1.64^{b}	73.79 ± 41.11^{a}	13.95 ± 1.96^{b}
ADP	9.48 ± 0.13^{c}	24.39 ± 0.11^{a}	19.89 ± 2.25^{b}
Cyclic AMP	6.70 ± 0.04^{a}	7.83 ± 0.49^{a}	10.33 ± 4.01^{a}
ATP	11.74 ± 0.44^{b}	76.04 ± 2.70^{a}	18.12 ± 8.96^{b}
Putrescine	7.77 ± 0.07^{b}	6.64 ± 0.12^{c}	12.31 ± 0.19^{a}
Betaine	11.29 ± 0.15^{b}	9.06 ± 0.33^{c}	16.94 ± 0.64^{a}
Anserine	4.59 ± 0.03^{a}	2.09 ± 0.23^{c}	3.69 ± 0.09^{b}
NAD	12.68 ± 0.26^{b}	9.31 ± 0.17^{c}	15.57 ± 0.22^{a}
NADP	8.28 ± 0.12^{c}	9.39 ± 0.31^{b}	13.91 ± 0.23^{a}

Within the row, values with different lowercase letters are significantly different ($P < 0.05$).

3.7. Pathway analysis

In order to analyse the disturbed pathways, principle metabolites were screened. The FCs of compounds under the combination of heat and AEW treatment are shown in Table 1. Fig. 7 presents the volcano plots based on correlation coefficients, *P* values, and FCs and the pathway analyses based on the screened metabolites. Metabolites with $P < 0.05$ and FCs >1.5 were recognised as statistically significant (Chen, Zhao, Wu, He, & Yang, 2020). As shown in Fig. 7A1-C1, there were 14, 11, and 8 metabolites located in the left sides of volcano plots, which indicated significantly decreased level of metabolites in SSA81, LM44, and LM3, respectively. Four amino acids (Val, Leu, Tyr, and Trp) reduced under the combined treatment in three *L. monocytogenes* strains. In contrast, only a few metabolites increased with FCs higher than 1.5 which were pointed in the right sides of the volcano plots. These statistically significant compounds may be recognised as makers for injured

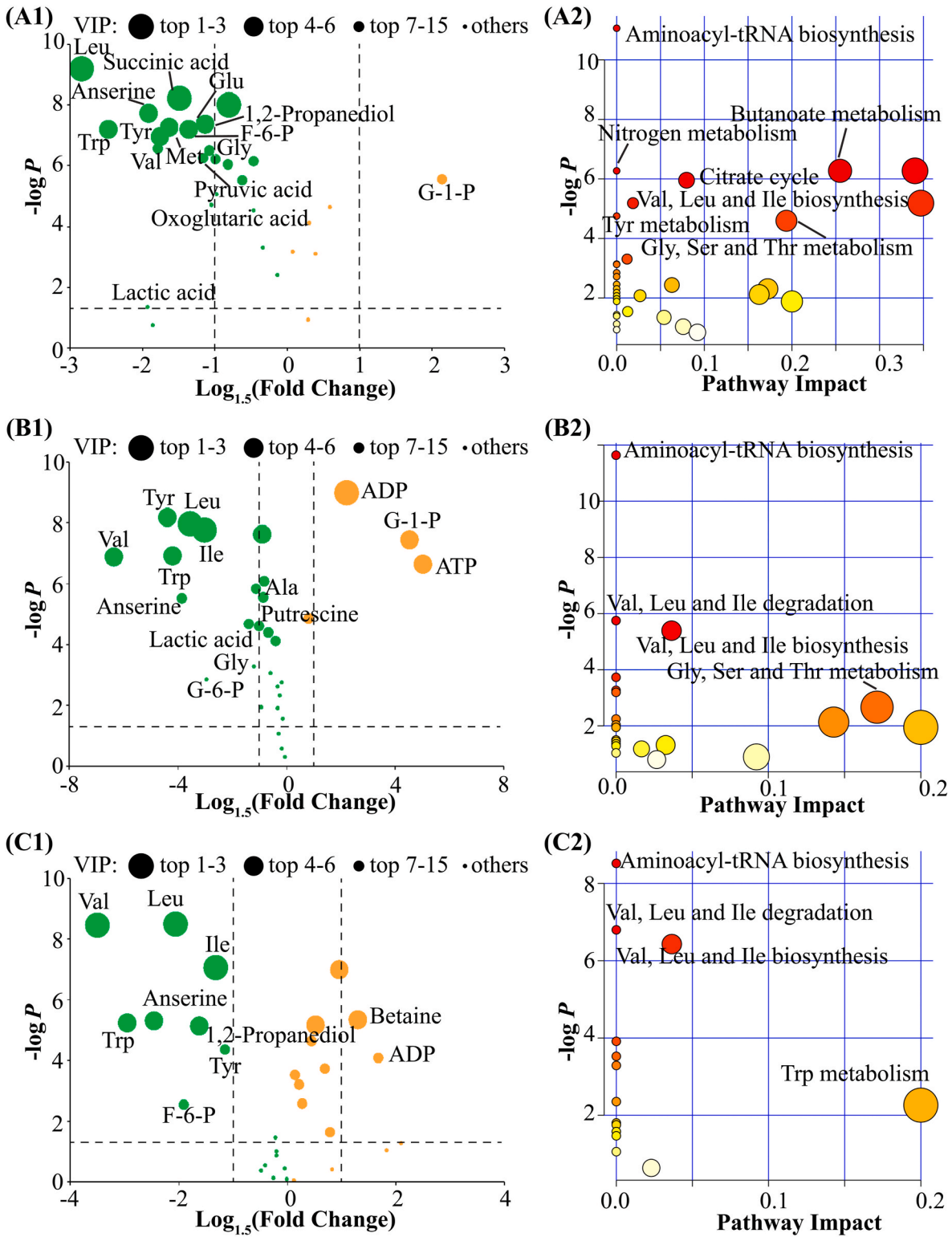

Fig. 7. Volcano plot of the control and combined treatment groups (A1-C1); pathway analysis for the control and combined treatment groups (A2-C2). Note: green colour in the volcano plot shows decreased amount after the combined treatment of heat and AEW; orange colour in the volcano plot shows increased amount after the combined treatment of heat and AEW. (For interpretation of the references to colour in this figure legend, the reader is referred to the Web version of this article.)

cells under the combined treatment.

Furthermore, pathway analysis was carried out based on screened metabolites and databases (Fig. 7A2-C2, Tables S4–S6). A total of 41, 22, and 14 pathways were predicted, with 15, 7, and 6 pathways had $P < 0.05$ for SSA81, LM44, and LM3, respectively. Disturbed pathways were mainly relevant to amino acid metabolism, energy metabolism, and carbohydrate metabolism. Five pathways, including aminoacyl-tRNA biosynthesis, Val, Leu, and Ile biosynthesis, Val, Leu, and Ile degradation, Phe, Tyr, and Trp biosynthesis, and novobiocin biosynthesis, were significantly changed for three *L. monocytogenes* strains under the combined treatment. For SSA81, ten more pathways (nitrogen metabolism, butanoate metabolism, Ala, Asp, and Glu metabolism, citrate

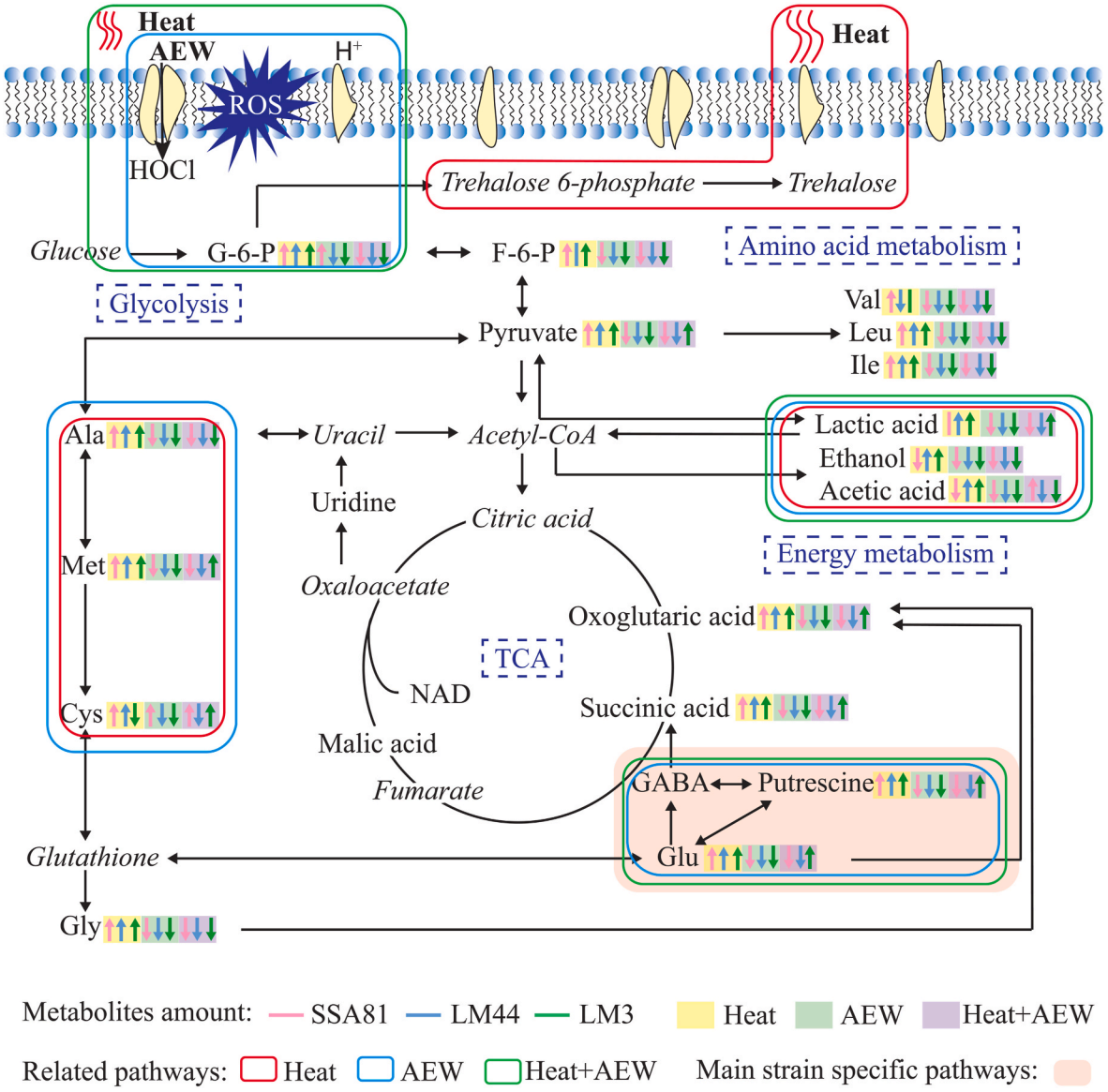

Fig. 8. Overview of metabolic alterations affected by the heat, AEW, and their combined treatment in three *Listeria monocytogenes* strains. Note: Upward and downward arrows beside metabolites indicate increased and decreased changes, respectively. No arrow indicates unchanged amount. Blue arrows: LM44; pink arrows: SSA81; green arrows: LM3. Metabolites in italic were not detected. Beside each metabolite, the yellow, green, and purple shadows under arrows indicate metabolite changes under heat, AEW, and the combined treatment, respectively. The main pathways affected by heat, AEW, and the combined treatment are circled in red, blue, and green boxes, respectively. Main strain specific pathways are shadowed by pink. (For interpretation of the references to colour in this figure legend, the reader is referred to the Web version of this article.)

cycle, pyruvate metabolism, Tyr metabolism, Gly, Ser, and Thr metabolism, glutathione metabolism, Phe metabolism, and pantothenate and CoA biosynthesis) were also significantly changed. For LM44, two more pathways, nitrogen metabolism and D-Ala metabolism, were significantly altered. Finally, for LM3, one more pathway, namely, Gly, Ser, and Thr metabolism was significantly altered. The number of significantly changed pathways revealed that the combined treatment had stronger effect on SSA81 than LM44 and LM3.

Based on KEGG and relative references, an assumptive schematic metabolic map was constructed to show the response of three *L. monocytogenes* strains under heat, AEW, and the combined treatment (Fig. 8). The mechanisms of individual treatment were that, as discussed in Section 3.4, bacterial protective systems were activated under heat treatment, while its metabolic flux was disrupted by AEW stress. Generally, in the combined treatment, the bactericidal effect of AEW was strengthened by heat, which might be due to the higher dynamic of active species in AEW. Initially, glucose is a preferable carbon and energy source for bacteria, which can be utilised in biosynthetic pathways and energy generation. As a pathway of sugar catabolism, glycolysis can provide biosynthetic precursors, such as glucose-6-phosphate and fructose-6-phosphate, and energy to cells (Doi, 2019). The reductions of essential biosynthetic precursors may be attributed to the disturbance of metabolic system. The decreased levels of ATP revealed that the combined treatment inhibited replenishment of energy for metabolic pathways.

In three *L. monocytogenes* strains, the depleted levels of Val, Leu, and Ile were detected. As major osmoregulation solutes, amino acids can preserve typical osmolality of cell ground substance and avoid disintegrate of subcellular compositions. However, Jozefczuk et al. (2010) reported that amino acids biosynthesis was sensitive to oxidative stress. In addition, high ORP and intolerable pH of AEW may damage membrane and induce osmotic imbalance (Chen et al., 2016). These reasons

explained the reductions of amino acids when the bacteria were treated with the combination of heat and AEW. Interestingly, some other amino acids, such as Ala, Met, Cys, Gly, and Glu, were also decreased in SSA81 and LM44 but increased in LM3, indicating that LM3 presented higher resistance and survival ability in response to the combined stress. The similar trends of betaine (data not shown) in three strains further verified our results. Betaine is a chemical chaperone synthesised from choline. It can maintain cell structural integrity and has been recognised as an osmoprotectant molecule (Gaucher et al., 2020).

As a key product of glycolysis, pyruvate is decarboxylated into acetyl-CoA, which involves in tricarboxylic acid cycle (TCA) and mixed acid fermentation. In SSA81 and LM44, the decreased amount of pyruvate caused the reductions of TCA related metabolites, such as oxoglutaric acid and succinic acid. It also led to the reductions of ethanol or acetic acid involved in mixed acid fermentation. The repression of both TCA cycle and mixed acid fermentation, and the associated damage of cellular function, even caused necrosis or apoptosis. Ye, Zhang, et al. (2012) reported that high temperature may reduce the dissolved oxygen in solution, thus the imbalance between offering and elimination of reactive oxygen species may increase oxidative stress when the cells under the combined treatment. Interestingly, the amount of oxoglutaric acid, succinic acid, ethanol, and acetic acid increased in LM3. This indicated that LM3 resisted the combined treatment of heat and AEW by activation of TCA cycle and mixed fermentation.

TCA cycle provides precursors and intermediates to other metabolic pathways, but it is also maintained by other metabolites. Therefore, the whole metabolic system can be influenced by the disturbance of one metabolic trajectory. For instance, Glu can synthesise γ-aminobutyrate (GABA) and further regulate succinic acid, which is involved in TCA cycle. The yield of GABA was reported as Glu decarboxylase system of bacteria, which enables cells to cope oxidative stress (Richard & Foster, 2004). GABA can be produced from putrescine, which serves as carbon and nitrogen source, and then used to generate succinate for maintenance of TCA cycle. The succinate produced by GABA may play a compensatory in overcoming TCA cycle inhibition. The reduced amount of Glu, succinate, and putrescine in SSA81 and LM44 revealed the diminishment of this compensatory pathway, whereas LM3 still struggled to overcome the combined stress even with higher amount of these compounds.

Overall, the disrupted synthesis and degradation pathways revealed the disturbance of anabolism and catabolism, respectively. The fluctuation of metabolites showed that the imbalance between catabolism and anabolism developed under the combined stress. This imbalance might lead to the loss of cell repair function and self-destruction of *L. monocytogenes*. In this case, *L. monocytogenes* remain viable and retain virulence but are unable to culture on agar.

4. Conclusion

The study investigated the bactericidal effect of heat, AEW, and their combination on *L. monocytogenes* strains inoculated on salmon, through comparing metabolic diversities of strains and global metabolic response to the treatments. Initially, the combined treatment was more effective than individual stress and induced 2.1–2.2 log CFU/g reductions. Overall, three *L. monocytogenes* strains showed similar metabolic profiles with 43 assigned metabolites. The heat treatment triggered protective systems in three *L. monocytogenes* strains, whereas AEW treatment attacked metabolic flux and dominated the combined treatment. However, the strain specific characteristics were presented by increased or decreased concentration of amino acids, organic acid, and nucleotides. There were 14, 11, and 8 metabolites significantly decreased in SSA81, LM44, and LM3 under the combined treatment, respectively. Further study illustrated that these changes might be due to the disturbance and alternation of the metabolic pathway of amino acid, energy, and carbohydrate, which were observed in three *L. monocytogenes* strains but at different extents. The numbers of significantly changed pathways for SSA81, LM44, and LM3 were 15, 7, and 6, respectively. The strain LM3 displayed the highest resistance to the combined treatment. This study showed that the bactericidal mechanisms could be explained by the disturbance of metabolic pathways, giving a direction for postprocessing sanitising. Besides, the *L. monocytogenes* metabolism can serve as a cornerstone for the symbiotic metabolism of microflora in food models.

CRediT authorship contribution statement

Jiaying Wu: Conceptualization, Methodology, Investigation, Software, Visualization, Writing - original draft. **Lin Zhao:** Methodology, Software, Resources, Validation. **Shaojuan Lai:** Writing - review & editing. **Hongshun Yang:** Conceptualization, Funding acquisition, Project administration, Supervision, Writing - review & editing.

Declaration of competing interest

The authors declare that they have no known competing financial interests or personal relationships that could have appeared to influence the work reported in this paper.

Acknowledgements

This study was funded by the Singapore Ministry of Education Academic Research Fund Tier 1 (R-160-000-A40-114), Natural Science Foundation of Jiangsu Province (BK20181184), and an industry project supported by Zhengzhou Bella Biotechnology Co., Ltd (R-160-000-B15-597).

Appendix A. Supplementary data

Supplementary data to this article can be found online at https://doi.org/10.1016/j.foodcont.2021.107974.

References

Alighialo, N. S., Rahimi, R., Hajirezaee, S., & Nikookhah, F. (2019). ^{1}H NMR-based metabolomics approach to understanding the temperature-dependent pathogenicity of *Lactococcus garvieae*. *International Journal of Aquatic Biology, 7*(4), 224–232. https://doi.org/10.22034/ijab.v7i4.609

Anon. (2013). Analysis of the baseline survey on the prevalence of *Listeria monocytogenes* in certain ready-to-eat foods in the EU, 2010–2011 Part A: *Listeria monocytogenes* prevalence estimates. *EFSA Journal, 11*(6), 3241. https://doi.org/10.2903/j.efsa.2013.3241

Bundy, J. G., Willey, T. L., Castell, R. S., Ellar, D. J., & Brindle, K. M. (2005). Discrimination of pathogenic clinical isolates and laboratory strains of *Bacillus cereus* by NMR-based metabolomic profiling. *FEMS Microbiology Letters, 242*(1), 127–136. https://doi.org/10.1016/j.femsle.2004.10.048

Cejka, C., Kubinova, S., & Cejkova, J. (2019). Trehalose in ophthalmology. *Histology & Histopathology, 34*(6), 611. https://doi.org/10.14670/HH-18-082

Chen, T. Y., Kuo, S. H., Chen, S. T., & Hwang, D. F. (2016). Differential proteomics to explore the inhibitory effects of acidic, slightly acidic electrolysed water and sodium hypochlorite solution on *Vibrio parahaemolyticus*. *Food Chemistry, 194*, 529–537. https://doi.org/10.1016/j.foodchem.2015.08.019

Chen, L., Zhao, X., Wu, J. E., He, Y., & Yang, H. (2020). Metabolic analysis of salicylic acid-induced chilling tolerance of banana using NMR. *Food Research International, 128*, 108796. https://doi.org/10.1016/j.foodres.2019.108796

Chen, L., Zhao, X., Wu, J. E., Liu, Q., Pang, X., & Yang, H. (2020). Metabolic characterisation of eight *Escherichia coli* strains including "Big Six" and acidic responses of selected strains revealed by NMR spectroscopy. *Food Microbiology, 88*, 103399. https://doi.org/10.1016/j.fm.2019.103399

Chhetri, V. S., Janes, M. E., King, J. M., Doerrler, W., & Adhikari, A. (2019). Effect of residual chlorine and organic acids on survival and attachment of *Escherichia coli* O157: H7 and *Listeria monocytogenes* on spinach leaves during storage. *Lebensmittel-Wissenschaft und -Technologie- Food Science and Technology, 105*, 298–305. https://doi.org/10.1016/j.lwt.2019.02.019

Diamant, S., Eliahu, N., Rosenthal, D., & Goloubinoff, P. (2001). Chemical chaperones regulate molecular chaperones in vitro and in cells under combined salt and heat stresses. *Journal of Biological Chemistry, 276*(43), 39586–39591. https://doi.org/10.1074/jbc.M103081200

Doi, Y. (2019). Glycerol metabolism and its regulation in lactic acid bacteria. *Applied Microbiology and Biotechnology, 103*(13), 5079–5093. https://doi.org/10.1007/s00253-019-09930-9

Dupre, J. M., Johnson, W. L., Ulanov, A. V., Li, Z., Wilkinson, B. J., & Gustafson, J. E. (2019). Transcriptional profiling and metabolomic analysis of *Staphylococcus aureus* grown on autoclaved chicken breast. *Food Microbiology, 82*, 46–52. https://doi.org/10.1016/j.fm.2019.01.004

Faleiro, M. L., Andrew, P. W., & Power, D. (2003). Stress response of *Listeria monocytogenes* isolated from cheese and other foods. *International Journal of Food Microbiology, 84*(2), 207–216. https://doi.org/10.1016/S0168-1605(02)00422-1

Gaucher, F., Rabah, H., Kponouglo, K., Bonnassie, S., Pottier, S., Dolivet, A., et al. (2020). Intracellular osmoprotectant concentrations determine *Propionibacterium freudenreichii* survival during drying. *Applied Microbiology and Biotechnology, 104*(7), 3145–3156. https://doi.org/10.1007/s00253-020-10425-1

Hati, S., Mandal, S., Minz, P. S., Vij, S., Khetra, Y., Singh, B. P., & Yadav, D. (2012). Electrolyzed oxidized water (EOW): Non-thermal approach for decontamination of food borne microorganisms in food industry. *Food and Nutrition Sciences, 3*(6), 760–768. https://doi.org/10.4236/fns.2012.36102

Heir, E., Solberg, L. E., Carlehög, M., Moen, B., Jensen, M. R., & Holck, A. L. (2020). Improved control of *Listeria monocytogenes* during storage of raw salmon by treatment with the fermentate Verdad N6 and nisin. *International Journal of Food Microbiology, 336*, 108895. https://doi.org/10.1016/j.ijfoodmicro.2020.108895

Huang, L. (2017). Dynamic kinetic analysis of growth of *Listeria monocytogenes* in a simulated comminuted, non-cured cooked pork product. *Food Control, 71*, 160–167. https://doi.org/10.1016/j.foodcont.2016.06.043

Huang, Y.-R., Hung, Y.-C., Hsu, S.-Y., Huang, Y.-W., & Hwang, D.-F. (2008). Application of electrolyzed water in the food industry. *Food Control, 19*(4), 329–345. https://doi.org/10.1016/j.foodcont.2007.08.012

Izumi, H., & Inoue, A. (2018). Viability of sublethally injured coliform bacteria on fresh-cut cabbage stored in high CO_2 atmospheres following rinsing with electrolyzed water. *International Journal of Food Microbiology, 266*, 207–212. https://doi.org/10.1016/j.ijfoodmicro.2017.11.028

Jiang, Y., Ai, C., Liao, X., Liu, D., & Ding, T. (2020). Effect of slightly acidic electrolyzed water (SAEW) and ultraviolet light illumination pretreatment on microflora inactivation of coriander. *Lebensmittel-Wissenschaft und -Technologie- Food Science and Technology, 132*, Article 109898. https://doi.org/10.1016/j.lwt.2020.109898

Josewin, S. W., Ghate, V., Kim, M.-J., & Yuk, H.-G. (2018). Antibacterial effect of 460 nm light-emitting diode in combination with riboflavin against *Listeria monocytogenes* on smoked salmon. *Food Control, 84*, 354–361. https://doi.org/10.1016/j.foodcont.2017.08.017

Jozefczuk, S., Klie, S., Catchpole, G., Szymanski, J., Cuadros-Inostroza, A., Steinhauser, D., et al. (2010). Metabolomic and transcriptomic stress response of *Escherichia coli*. *Molecular Systems Biology, 6*, 364. https://doi.org/10.1038/msb.2010.18

Kong, F., Tang, J., Rasco, B., Crapo, C., & Smiley, S. (2007). Quality changes of salmon (*Oncorhynchus gorbuscha*) muscle during thermal processing. *Journal of Food Science, 72*(2), S103–S111. https://doi.org/10.1111/j.1750-3841.2006.00246.x

Krajnik, M. M., Feng, L. X. J., Bang, W. S., & Yuk, H.-G. (2017). Inactivation of *Listeria monocytogenes* and natural microbiota on raw salmon fillets using acidic electrolyzed water, ultraviolet light or/and ultrasounds. *Food Control, 74*, 54–60. https://doi.org/10.1016/j.foodcont.2016.11.033

Lan, L., Zhang, R., Zhang, X., & Shi, H. (2019). Sublethal injury and recovery of *Listeria monocytogenes* and *Escherichia coli* O157:H7 after exposure to slightly acidic electrolyzed water. *Food Control, 106*, 106746. https://doi.org/10.1016/j.foodcont.2019.106746

Len, S.-V., Hung, Y.-C., Erickson, M., & Kim, C. (2000). Ultraviolet spectrophotometric characterization and bactericidal properties of electrolyzed oxidizing water as influenced by amperage and pH. *Journal of Food Protection, 63*(11), 1534–1537. https://doi.org/10.4315/0362-028X-63.11.1534

Liao, L. B., Chen, W. M., & Xiao, X. M. (2007). The generation and inactivation mechanism of oxidation–reduction potential of electrolyzed oxidizing water. *Journal of Food Engineering, 78*(4), 1326–1332. https://doi.org/10.1016/j.jfoodeng.2006.01.004

Li, S., Tian, Y., Jiang, P., Lin, Y., Liu, X., & Yang, H. (2020). Recent advances in the application of metabolomics for food safety control and food quality analyses. *Critical Reviews in Food Science and Nutrition*. https://doi.org/10.1080/10408398.2020.1761287 (in press).

Liu, Q., Chen, L., Laserna, A. K. C., He, Y., Feng, X., & Yang, H. (2020). Synergistic action of electrolyzed water and mild heat for enhanced microbial inactivation of *Escherichia coli* O157:H7 revealed by metabolomics analysis. *Food Control, 110*, 107026. https://doi.org/10.1016/j.foodcont.2019.107026

Liu, Q., Tan, C. S. C., Yang, H., & Wang, S. (2017). Treatment with low-concentration acidic electrolysed water combined with mild heat to sanitise fresh organic broccoli (*Brassica oleracea*). *Lebensmittel-Wissenschaft und -Technologie- Food Science and Technology, 79*, 594–600. https://doi.org/10.1016/j.lwt.2016.11.012

Liu, Q., Wu, J. E., Lim, Z. Y., Aggarwal, A., Yang, H., & Wang, S. (2017). Evaluation of the metabolic response of *Escherichia coli* to electrolysed water by 1 H NMR spectroscopy. *LWT-Food Science and Technology, 79*, 428–436. https://doi.org/10.1016/j.lwt.2017.01.066

Liu, Q., Wu, J. E., Lim, Z. Y., Lai, S., Lee, N., & Yang, H. (2018). Metabolite profiling of *Listeria innocua* for unravelling the inactivation mechanism of electrolysed water by nuclear magnetic resonance spectroscopy. *International Journal of Food Microbiology, 271*, 24–32. https://doi.org/10.1016/j.ijfoodmicro.2018.02.014

Lokerse, R. F. A., Maslowska-Corker, K. A., van de Wardt, L. C., & Wijtzes, T. (2016). Growth capacity of *Listeria monocytogenes* in ingredients of ready-to-eat salads. *Food Control, 60*, 338–345. https://doi.org/10.1016/j.foodcont.2015.07.041

Lou, X., Zhai, D., & Yang, H. (2021). Changes of metabolite profiles of fish models inoculated with Shewanella baltica during spoilage. *Food Control, 123*, 107697. https://doi.org/10.1016/j.foodcont.2020.107697

Lungu, B., Ricke, S. C., & Johnson, M. G. (2009). Growth, survival, proliferation and pathogenesis of *Listeria monocytogenes* under low oxygen or anaerobic conditions: A review. *Anaerobe, 15*(1–2), 7–17. https://doi.org/10.1016/j.anaerobe.2008.08.001

MacIntyre, A. M., Barth, J. X., Pellitteri Hahn, M. C., Scarlett, C. O., Genin, S., & Allen, C. (2020). Trehalose synthesis contributes to osmotic stress tolerance and virulence of the bacterial wilt pathogen *Ralstonia solanacearum*. *Molecular Plant-Microbe Interactions, 33*(3), 462–473. https://doi.org/10.1094/MPMI-08-19-0218-R

Miya, S., Takahashi, H., Ishikawa, T., Fujii, T., & Kimura, B. (2010). Risk of *Listeria monocytogenes* contamination of raw ready-to-eat seafood products available at retail outlets in Japan. *Applied and Environmental Microbiology, 76*(10), 3383–3386. https://doi.org/10.1128/AEM.01456-09

Park, J.-S., & Ha, J.-W. (2020). Synergistic antimicrobial effect of X-ray and curcumin against *Listeria monocytogenes* on sliced cheese. *Food Control, 110*, 106986. https://doi.org/10.1016/j.foodcont.2019.106986

Richard, H., & Foster, J. W. (2004). *Escherichia coli* glutamate-and arginine-dependent acid resistance systems increase internal pH and reverse transmembrane potential. *Journal of Bacteriology, 186*(18), 6032–6041. https://doi.org/10.1128/JB.186.18.6032-6041.2004

Schjørring, S., Lassen, S. G., Jensen, T., Moura, A., Kjeldgaard, J. S., Müller, L., & Nielsen, E. M. (2017). Cross-border outbreak of listeriosis caused by cold-smoked salmon, revealed by integrated surveillance and whole genome sequencing (WGS), Denmark and France, 2015 to 2017. *Euro Surveillance, 22*(50), Article 17-00762. https://doi.org/10.2807/1560-7917.ES.2017.22.50.17-00762

Shen, C., Lemonakis, L., Etienne, X., Li, K., Jiang, W., & Adler, J. M. (2019). Evaluation of commercial antimicrobials against stress-adapted *Campylobacter jejuni* on broiler wings by using immersion and electrostatic spray and an economic feasibility analysis. *Food Control, 103*, 161–166. https://doi.org/10.1016/j.foodcont.2019.04.013

Shiroodi, S. G., Ovissipour, M., Ross, C. F., & Rasco, B. A. (2016). Efficacy of electrolyzed oxidizing water as a pretreatment method for reducing *Listeria monocytogenes* contamination in cold-smoked Atlantic salmon (*Salmo salar*). *Food Control, 60*, 401–407. https://doi.org/10.1016/j.foodcont.2015.08.020

Singh, A. K., Ulanov, A. V., Li, Z., Jayaswal, R. K., & Wilkinson, B. J. (2011). Metabolomes of the psychrotolerant bacterium *Listeria monocytogenes* 10403S grown at 37 °C and 8 °C. *International Journal of Food Microbiology, 148*(2), 107–114. https://doi.org/10.1016/j.ijfoodmicro.2011.05.008

Todd, E. C. D., & Notermans, S. (2011). Surveillance of listeriosis and its causative pathogen, *Listeria monocytogenes*. *Food Control, 22*(9), 1484–1490. https://doi.org/10.1016/j.foodcont.2010.07.021

Wang, L., & Shen, C. (2015). Survival of unstressed and acid-, cold-, and starvation-stress-adapted *Listeria monocytogenes* in ham extract with hops beta acids and consumer acceptability of HBA on ready-to-eat ham. *BioMed Research International*, 817042. https://doi.org/10.1155/2015/817042. *2015*.

Wu, S. T., Burnett, J., Wang, J., Hammons, S. R., Veenhuizen, D. R., & Oliver, H. F. (2020). Infrastructure, sanitation, and management practices impact *Listeria monocytogenes* prevalence in retail grocery produce environments. *Food Control, 109*, 106911. https://doi.org/10.1016/j.foodcont.2019.106911

Ye, Y., Wang, X., Zhang, L., Lu, Z., & Yan, X. (2012). Unraveling the concentration-dependent metabolic response of *Pseudomonas* sp. HF-1 to nicotine stress by 1H NMR-based metabolomics. *Ecotoxicology, 21*(5), 1314–1324. https://doi.org/10.1007/s10646-012-0885-4

Ye, Y., Zhang, L., Hao, F., Zhang, J., Wang, Y., & Tang, H. (2012b). Global metabolomic responses of *Escherichia coli* to heat stress. *Journal of Proteome Research, 11*(4), 2559–2566. https://doi.org/10.1021/pr3000128

Zhao, X., Chen, L., Wu, J. E., He, Y., & Yang, H. (2020). Elucidating antimicrobial mechanism of nisin and grape seed extract against *Listeria monocytogenes* in broth and on shrimp through NMR-based metabolomics approach. *International Journal of Food Microbiology, 319*, 108494. https://doi.org/10.1016/j.ijfoodmicro.2019.108494

Zhao, X., Wu, J. E., Chen, L., & Yang, H. (2019c). Effect of vacuum impregnated fish gelatin and grape seed extract on metabolite profiles of tilapia (*Oreochromis niloticus*) fillets during storage. *Food Chemistry, 293*, 418–428. https://doi.org/10.1016/j.foodchem.2019.05.001

Zhao, L., Zhang, Y., & Yang, H. (2017). Efficacy of low concentration neutralised electrolysed water and ultrasound combination for inactivating *Escherichia coli* ATCC 25922, *Pichia pastoris* GS115 and *Aureobasidium pullulans* 2012 on stainless steel coupons. *Food Control, 73*, 889–899. https://doi.org/10.1016/j.foodcont.2016.09.041

Zhao, L., Zhao, M. Y., Phey, C. P., & Yang, H. (2019a). Efficacy of low concentration acidic electrolysed water and levulinic acid combination on fresh organic lettuce (*Lactuca sativa Var. Crispa* L.) and its antimicrobial mechanism. *Food Control, 101*, 241–250. https://doi.org/10.1016/j.foodcont.2019.02.039

Zhao, L., Zhao, X., Wu, J. E., Lou, X., & Yang, H. (2019b). Comparison of metabolic response between the planktonic and air-dried Escherichia coli to electrolysed water combined with ultrasound by 1H NMR spectroscopy. *Food Research International, 125*, 108607. https://doi.org/10.1016/j.foodres.2019.108607

Zhu, M., Du, M., Cordray, J., & Ahn, D. U. (2005). Control of *Listeria monocytogenes* contamination in ready-to-eat meat products. *Comprehensive Reviews in Food Science and Food Safety, 4*(2), 34–42. https://doi.org/10.1111/j.1541-4337.2005.tb00071.x